# Experimental characterization of spray-wall interaction under cross-flow conditions

**Panão, M.R.O., Moreira A.L.N.**

Instituto Superior Técnico, Dep. Mech. Eng., Lisbon, PORTUGAL

This paper reports an experimental study on the impingement of an intermittent gasoline spray onto a flat surface in the presence of a cross flow. The experiments include detailed PDA measurements of droplet size, velocity and volume flux in the vicinity of the wall, which are analysed in terms of the time dependent fluid-dynamic interactions between the spray, the wall and the cross flow.

## Introduction

Regardless the fuel-air mixing strategy used in a spark ignition internal combustion engine (either Direct-Injection Stratified Charge, DISC, or in Port-Fuel Injected, PFI), impingement of the fuel spray onto interposed surfaces affects the performance of the engine. The quality of the combustible mixture in the vicinity of the spark plug at the time of ignition and, therefore, combustion efficiency, depends on complex thermo-fluid-dynamic interactions between the liquid droplets and their vapor with the surrounding air and solid surfaces. In addition, at cold start, a fuel film would prevail at the impact surfaces, thus making it necessary to supply amounts of fuel exceeding those required for the ideal mixture ratio. As a result, the engine experiences an unstable burn with an associated significant increase in the emissions of unburned hydrocarbons [1, 2]. A better understanding of the interaction mechanisms is required if engine performance is to be improved and is the objective of our work. However, the present study considers a gasoline injection system operating at the low pressure of injections typical of port-injection engines.

Several experiments are reported in the literature, which consider the interaction mechanisms in simplified laboratory configurations where some of the complexities of practical flow were removed. For example, Brunello *et al.* [4] observed that the main influence of a cross flow on a transient Diesel spray is to alter the distributions of droplet size and velocity due to selective effect of drag, but did not considered impingement. When a surface is interposed, the influence of the cross flow is to alter the conditions (size, normal velocity, angle and flux) of droplets at impact, as reported by Arcoumanis and Cutter [5]. A secondary effect of the wall is due to the formation of a wall-jet vortex [5], which moves smaller droplets off the wall after impingement, to be entrained by the cross flow. The authors also report on the complex interaction between the cross flow and the vortical structure. Later, Arcoumanis *et al.* [6] considered the effects of a pre-existing liquid film, so their work contribute to better understanding the consequences of spray impingement as is known in PFI intake ports in cold-start conditions. Their results suggest that the thickness of the wall-film is decreased by the cross-flow, which makes the size of droplets produced by secondary atomization to decrease. As a consequence, the distribution of post-impinged droplets, which interact with the vortical structure at the wall, also includes secondary droplets due to film stripping besides those due to splash and/or rebound.

Despite their important contribution, previous works seldom report measurements close enough to the wall, from which the wall interaction mechanisms may be inferred. Therefore, those mechanisms are usually modeled based on experiments with single drops, which are extrapolated to a poly-dispersed spray situation by summing over all the size distribution [7 – 9]. However, this procedure has been shown to be inaccurate [10] and a detailed characterization of the distributions of the impinging and post-impinging droplets is still required. This is the objective of the study reported here.

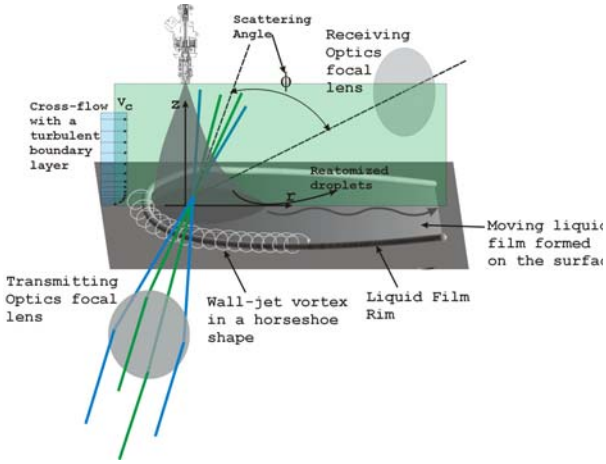


**Figure 1** Spray impact on a flat plate in the presence of a cross-flow and optical configuration of the 2D phase-Doppler system used in the experiments.

The flow configuration considered in this work is that of a gasoline spray impinging onto a flat plate through a cross-flow of air as shown in Figure 1. The aerodynamic forces created by the cross flow distort the wall inducing shear forces, which make the fuel film to develop in a horseshoe shape with an outer rim and dimples inside. The measurements follow those reported in Panão and Moreira [11, 12], where the global structure of the spray directed 90º to the surface in the presence of a cross-flow was visualized for different injection pressures, using a Mie scattering and a shadow-graphic technique to distinguish between the liquid gasoline and its vapor. The influence of the cross-flow in altering droplet dispersion before and after impact was shown to be qualitatively consistent with observations by other authors and the follow-up of this work is to provide detailed measurements close to the wall, which may characterize spray/wall interactions.

## The experimental method

The experimental configuration is described in detail in Panão and Moreira [11, 12] and only a summary is given here: the spray issues from a commercial pintle-type injector used in PFI gasoline engines with a pintle diameter of 0.79 mm inserted in a cylindrical hole with 0,9 mm in diameter. The injector is placed vertically faced downwards at the top of the working section of a wind tunnel (270 mm long, 150 mm wide) and sprays through a cross stream of air perpendicularly onto the bottom surface, which is located at 50 mm. The side walls of the working section are made of glass to provide optical acess to the flow and the target surface is made of aluminium with a mean roughness of 2.5μm. The fluid used is commercial gasoline, which properties were measured to be: density, 749.6 kg/m$^3$; viscosity, $4.2612\times10^{-4}$ kg/m/s; refractive index, 1.44 and surface tension 19.4 mN/m.

The injector solenoid is triggered by a TTL pulse controlled by a function generator board, NI5411 from National Instruments, which allows varying the injection frequency, duration and the number of cycles. The injection pressure is manually controlled with a pressure regulation valve. The experiments reported here were obtained with a pressure of injection of 3 bar, a duration and frequency of injection of 10 ms and 10 Hz (≈ 1200 rpm), respectively, which correspond to a volume flow rate of 12 liters/h. The cross flow of air was set at a bulk velocity of 11 m/s with a temperature of 25ºC (± 2ºC).

Local time-resolved measurements of droplet size, velocity and flux are simultaneously measured with a two-component phase Doppler DANTEC system consisting of a 55X

transmitting optics, a 57x10 PDA receiving optics and a 58N10 Covariance processor. Phase resolved measurements are performed using the built-in software for rotating machinery. The TTL signal used to trigger the injector is used as a phase reference to tag the data during data acquisition. Phase-locked measurements are obtained within a phase window of $1{,}8^{o}$, which corresponds a duration of 500 μs. The number of cycles used to form the conditional measurements depends on the total number of samples required by the signal processor and on the number of samples acquired during each window, which in turn depends on the rate of droplets passing through the control volume leading to a validated Doppler burst. For the flow conditions considered here and for a population of 60000 samples, the number of cycles used to form the phase averages is usually over 2000. Size dependent measurements are obtained by processing the Doppler signals within size bins of 10μm. Statistical uncertainties in each size bin were estimated for all phase averages, and were always less than 6% and 13% for the mean and rms velocities, [13] and less than 10% for the SMD, [14].

The complete PDA system is fixed and the test section is mounted on a three-dimensional traversing unit, allowing the positioning of the laser control volume within ±0.25mm. The measurements reported here were obtained within the vertical plan of symmetry, as shown in Figure 1, to avoid as much as possible a misinterpretation of the normal velocity component, since the flow is actually tri-dimensional. The origin of the axial coordinate, $z$, is taken at the impinging surface and the origin of the transverse coordinate, $r$, is taken at the axis of the injector; the axial velocity, $U$, is positive downwards and the transverse velocity, $V$, is positive in the direction of the cross flow.

**Results and Discussion**

In the following, all spatial coordinates are made non-dimensional by the circular hole of the injector, $D = 0.9\ mm$, and all velocities are made non-dimensional by the corresponding bulk velocity, defined as $U_o = Q/(\Delta t\ A_s)$, where $Q$ is the volume of gasoline supplied during an entire cycle, $\Delta t$ is the cycle duration and $A_S$ is the area of the injector based on $D$. For the flow conditions reported here $U_o = 22.8\ m/s$. The interaction between the spray, the cross flow and the wall is inferred by comparing measurements made in the unconfined non-impinging spray (FS) with measurements made in the impinging sprays without cross flow (SI) and with cross flow (SIWCF). The analysis is performed at three points at the same axial station in each flow (see Figure 2) chosen to be upstream, at and downstream the axis of the injector. The axial station is at $z/D = 7.8$ (7 mm from the wall), which is the smallest distance the control volume can approach the target wall without blocking the laser beams in the vertical plane.

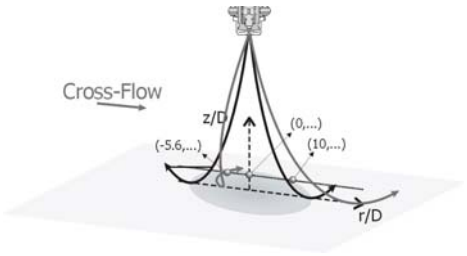


**Figure 2** Location of the measurement points.

The consequences of spray impact can be analyzed from the $V/U_0$ - $U/U_0$ correlations at the axis of symmetry shown in Figure 3. Each point in the plots refer to an individual droplet; a positive axial velocity component denotes a droplet moving towards the surface and a negative axial velocity a droplet moving away from the surface due to, either, total rebound or re-atomization. Since the measurements reported here were made at ambient temperature (which may correspond to cold-start conditions), the dominant mechanisms of secondary atomization are expected to be rebound, splash and film striping when the cross-flow is present [7]. Depending on the mechanism, these droplets may move with different directions.

While the obvious effect of the wall is the occurrence of a secondary atomization, that of the cross-flow is to alter droplets dispersion due aerodynamic drag forces exerted upon the spray. As a result, not only the size and velocity distributions of impinging droplets is altered, but also the trajectory of the post-impinging droplets is altered from what was expected in quiescent surroundings.

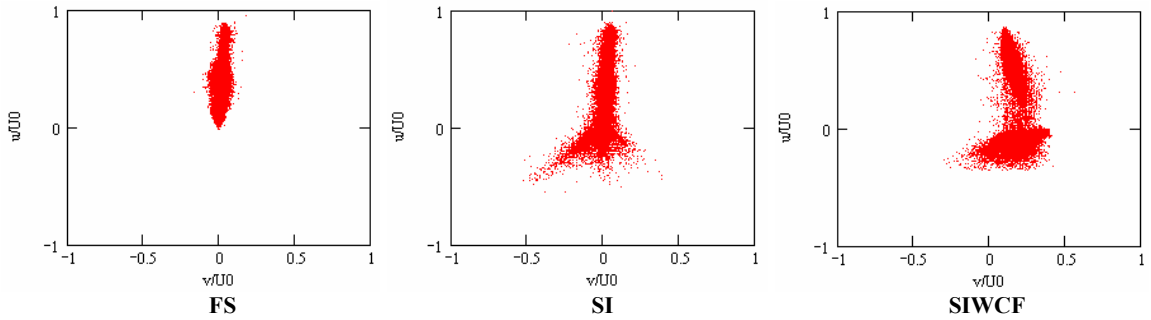


**Figure 3** Correlations between the dimensionless time averaged axial and radial velocity components at r/D = 0 for FS, SI and SIWCF.

It is worth mentioning that the results represented in Figure 3 refer to velocities averaged over the entire cycle. However, the spray is transient and, therefore the impact conditions may vary during the cycle. It is expected that the behavior of each droplet at impact may be influenced by the behavior of all other droplets, which had impinged differently before. The transient nature of the free spray (FS) is depicted in Figure 4 at *r/D = -5.6* for droplets within three size classes centered at 20μm, 50μm and 70μm, respectively.

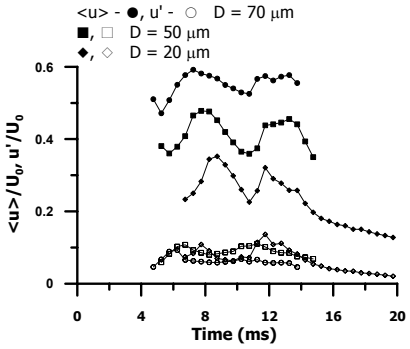


**Figure 4** Time variation of the axial velocity for three droplet size classes at r/D = -5.6.

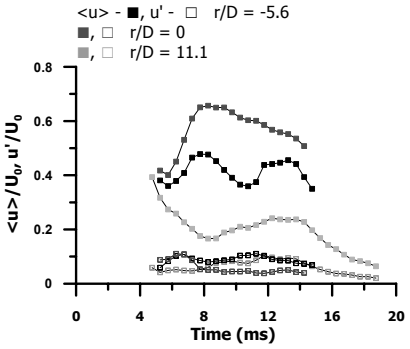


**Figure 5** Time variation of the axial velocity of 50μm droplets at r/D = (-5.6; 0; 11.1) for the FS case.

The opening of the pintle gives rise to a pressure wave inside the fuel line, originating velocity modulations in the subsequent free liquid sheet [15]; these perturbations cause the observed periodic behavior of droplet velocity, which is attenuated as droplet size increases. However, the trends of the perturbations are not similar within the cross-sectional area of the spray, as shown in Figure 5: the magnitude of the axial velocity is similar at all radial locations at the initial instant at which droplets are firstly detected; droplets at the centerline experience a large positive velocity gradient up to *t = 8 ms*, from which the velocity starts to decrease with no periodicity until *t = 14 ms* where the end-of-injection (EOI) occurs; but droplets at *r/D = 11.1* show the opposite trend. Therefore, the impact energy of droplets available at impact for

secondary atomization is not uniform, but varies in time with a larger amplitude around the centerline and decreasing away from it.

The interposition of a wall gives rise to the formation of a wall-jet vortex with a donut shape, as a result of the air entrainment into the spray core induced by the dynamic vacuum characteristic of a spray with a hollow-cone structure [16]. This vortex breaks into numerous vortices [12, 17] and is convected away from the centerline, slowly expanding its average radius in time as more air is entrained into the structure. Figure 6 shows a photograph of the flow with the relative location of the measuring points within the referred structure.

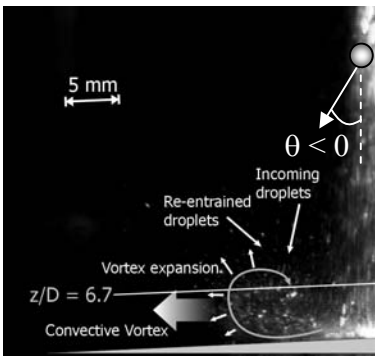


**Figure 6** Representation of the re-entrainment of droplets due to the vortical flow induced by the wall.

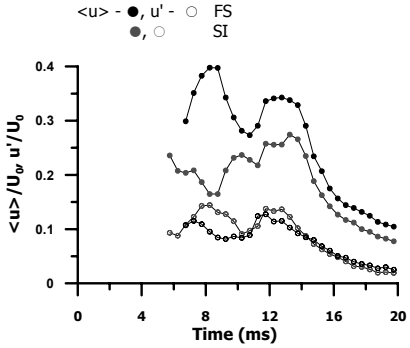


**Figure 7** Time variation of the axial velocity of 40μm droplets for FS and SI at r/D = -5.6.

The influence of the wall on the transient behavior of droplets at impact is shown in Figure 7 for the 40μm droplets at *r/D = 5.6*, where the phase averaged and fluctuating velocities are compared for the FS and SI cases. In general, the results show phase averaged axial velocities are larger in the free spray (FS), denoting that the presence of the wall decreases the penetration rate of the spray. Therefore, the energy available at impact is smaller than it was expected from the analysis of the free spray. Further, although time variations of the axial velocity still occur for the SI case, they do not show any definite periodicity, which may be due to the contribution of re-impingement of the re-atomized droplets entrained by the vortical structure. The net effect of the transient nature on droplet characteristics at impact still requires knowledge of the volume flux of droplets impinging at each radial location. At this point, it must be recalled that the average volume flux is smaller at *r/D = 0* due to the hollow structure of the spray and at *r/D = 11.0* which corresponds to a point outside the edge of the spray.

The cross-flow creates an additional aerodynamic drag force to enhance momentum exchange between the gaseous-phase and the spray. Smaller droplets, which are more responsive, are dragged away by the cross flow before they attain the surface, so that is why at *r/D = -5.6* the overall mean diameter is larger and a reasonable number of smaller droplet were not detected. Therefore, we choose the 80 μm droplets to compare the time variation of the axial velocity for the three cases (FS, SI and SIWCF) as shown in Figure 8. The substantial reduction of the axial velocity measured along time, accompanied by an increase of the radial component, suggest that droplet trajectory is altered not only by the cross flow, but also by the wall boundary layer, which may induce an additional transverse force due to shear (Saffman lift force), as also observed by [18].

The influence of the cross flow on impingement is better characterized by the angle, θ, between the normal to the surface and the direction of the re-atomized droplet as shown in Figure 9 for the size classes centered at 30, 40 and 50 μm. Here, post-impinged droplets have been identified by the negative signal of the velocity component perpendicular to the wall, *U*. As expected, re-atomization scarcely occurs at the centerline of the free spray (FS) where

droplets impinge normally to the surface during most of the time. In fact, droplets moving away from the surface after impingement could only be detected for *3 ms* ASOI and may be due to re-atomization of larger droplets impinging at surrounding positions.

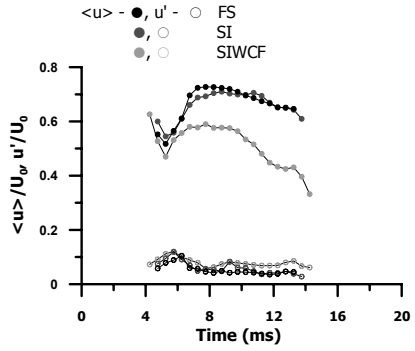


**Figure 8** Time variation of axial velocity of the 80μm droplets for FS, SI and SIWCF at r/D = 0.

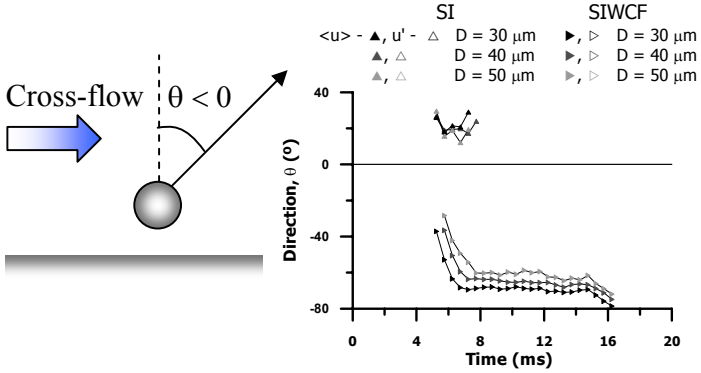


**Figure 9** Time variation of the direction of post-impinged droplets at r/D = 0, for FS, SI and SIWCF.

The cross flow alters this behavior and three periods of time can be identified: the former extends up to about *3 ms* during which θ increases very fast to large absolute angles; the second lasts up to about *7 ms*, during which droplet trajectories attain a steady state and leave the surface with a very large angle; the third lasts up to EOI – droplets trajectory become almost parallel to the wall. This behavior does not change qualitatively with droplet size and quantitative differences may be attributed to different response times. However, it is worth mentioning at this point, that the observed effects of the cross flow may not be analyzed solely in terms of momentum exchange with the cross flow, but also in terms of the contribution of the cross stream to the mechanisms of interaction of individual droplets with the surface. That is, splash, rebound and stripping of the liquid film, which may give rise to different trajectories of the re-atomized droplets, may now be altered by the cross flow.

The regime followed by each droplet in the spray depends on the ratio between the several forces acting upon the droplet at impact: inertia, surface tension and viscous forces. Those forces are usually scaled based on non-dimensional numbers, such as the Reynolds number, $Re = (U_o \cdot D_o)/\nu$; the Weber number, $We = (\rho \cdot U_o^2 \cdot D_o)/\sigma$; and Ohnesorge number, $Oh = (We)^{0.5}/Re$. The transition between regimes is then modeled by critical values described as functions of some or all of those numbers. From the numerous models reported in the literature, three were applied to the measurements reported here: [7], [9] and [19]. The Ohnesorge and Reynolds numbers were calculated based on the PDA measurements and the results from *4ms* up to *16 ms* ASOI plotted in Figures 10 and 11, where the empirical correlations are also depicted. Four shadowed regions denote the regimes of adhesion, rebound, spread or splash, respectively. For the later, a transition region is considered instead of a line, since the splash criteria vary depending if the surface is dry or wetted, or if the liquid film is thin or thick. Figure 10 refers to SI, while Figure 11 refers to SIWCF. In general, the results show that, after *9 ms* ASOI, a significant number of droplets in the SI are predicted to stick. Droplets within this regime have a low impact energy, which is the case of smaller secondary droplets, which are re-entrained by the vortex and re-impinge. In practice, it is expected that these droplets contribute to increase the liquid film formed by droplets in the spread regime. Splash becomes a relative more important mechanism at *9* and *12 ms* ASOI, and almost disappears at *16 ms*, when the injector is already closed and impinging droplets are re-atomized droplets which remained suspended by the secondary air motions.

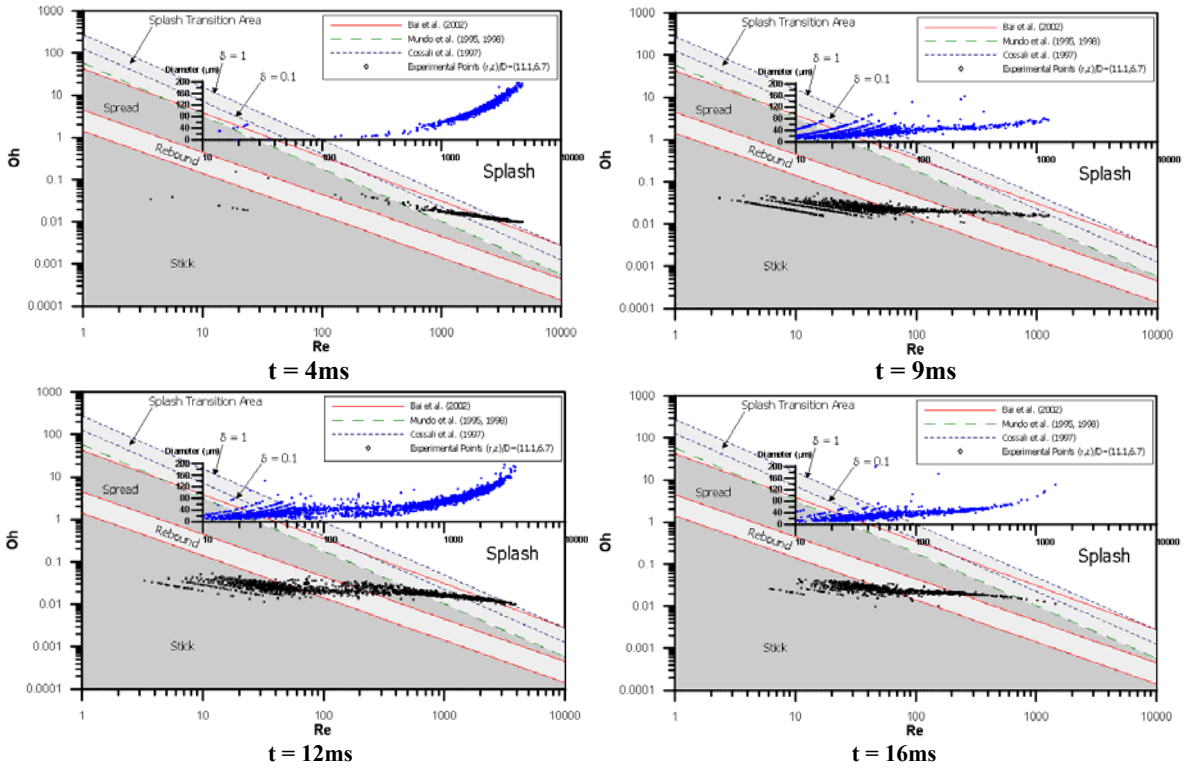


**Figure 10** Transition regimes predicted for impinging droplets within each time window for SI at r/D = 11.1

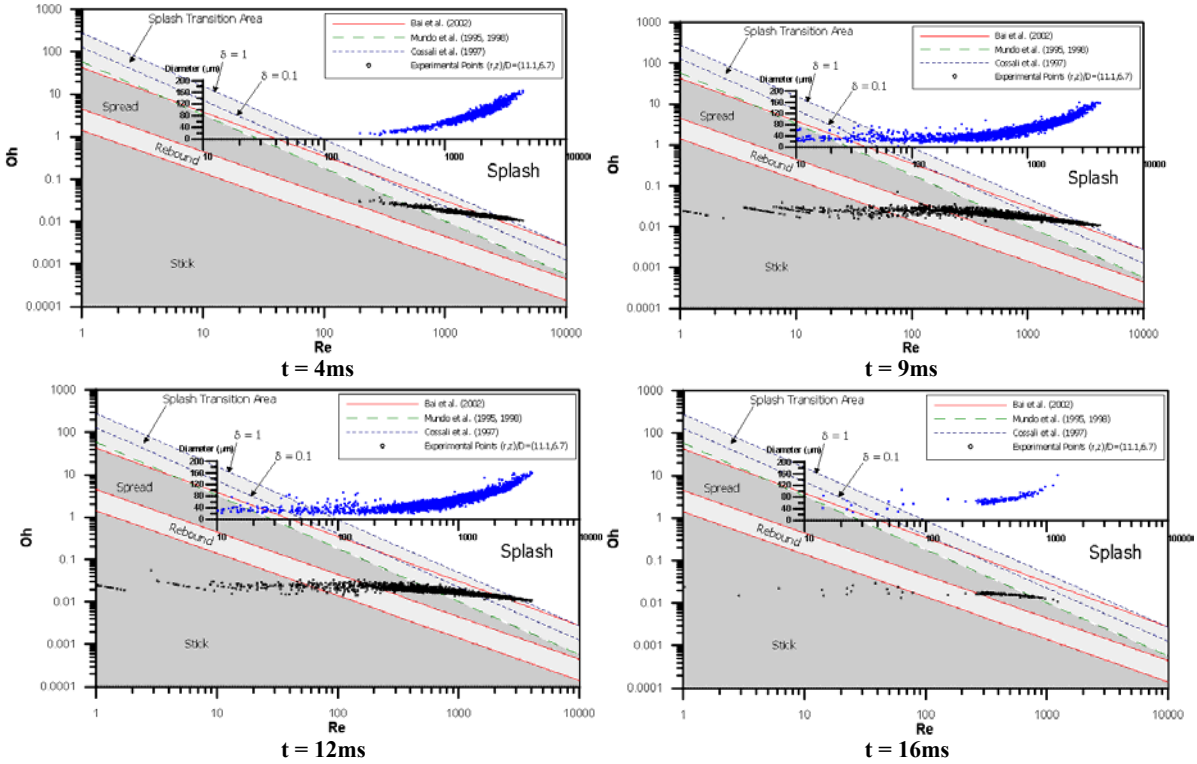


**Figure 11** Transition regimes predicted for impinging droplets within each time window for SIWCF at r/D = 11.1

Figure 11 shows that the cross flow decreases the number of droplets in the stick regime, which is consistent with the fact that the cross flow convects the responsive secondary droplets initially re-entrained by the vortical structure, thus avoiding their re-impingement.

For easy of analysis, the plots in Figures 10 and 11 also include the variation of the impact Reynolds number with droplet diameter. These curves show that another clear effect of the cross flow is to give rise to a comparatively larger number of droplets impinging with large Reynolds number at *9 ms* ASOI. As a consequence, splash becomes an increasingly important mechanism. Finally, with cross flow, less droplets remain suspended after the end of injection at *16 ms* and only a few were detected.

**Summary**

This paper reports an experimental study on the impingement of an intermittent gasoline spray onto a flat surface in the presence of a cross flow. The experiments include detailed PDA measurements of droplet size, two velocity components and volume flux in the vicinity of the wall, and are aimed at understanding the time dependent fluid-dynamic interactions between the spray, the wall and the cross flow. The main effect of the wall is due to the formation of a three-dimensional vortical structure in the vicinity of the wall, which entrains re-atomized droplets to re-impinge with smaller Reynolds numbers, thus contributing to the formation of the wall liquid film. Although spray/wall interaction mechanisms are altered due to deviation of the impinging spray by the cross flow, the main effect is due to drag of small droplets from the vortical structure thus reducing the number of droplets predicted to stick at the wall.

**Acknowledgments**

The authors thank Mr. John Laker of Imperial College of Science, Technology and Medicine of the University of London, for his valuable support in designing and building the fuel injection system. The authors also acknowledge the contribution of the National Foundation of Science and Technology of the Ministry for Science and Technology by supporting this study through the project POCTI/ 1999/ EME/ 38082 and by supporting M. R. Panão with a Research Grant.

**References**

[1] Zhao F-Q, Lai M-C and Harrington D L *SAE Technical Paper* 950506
[2] Kelly-Zion P L, Styron J P, Lee C F, Lucht R P, Peters J E and White R A 2000 *Atomization and Sprays* **10** 1-23
[3] Zhao F-Q, Takemoto M, Nishida K, Hiroyasu H 1992 *SAE Technical Paper* 922389
[4] Brunello G, Coghe A, Cossali G E and Gamma F 1990 *5th Int. Symp. Appl. Laser Tech. Fluid Mech.* Lisbon, Portugal
[5] Arcoumanis C and Cutter P 1995 *SAE Technical Paper* 950448
[6] Arcoumanis C, Whitelaw D S and Whitelaw J H 1997 *Atom. and Sprays* **7** 437-456
[7] Mundo C, Sommerfeld M and Tropea C 1995 *Int. J. Multiphase Flow* **21** 81-173
[8] Yarin A L and Weiss D A 1995 *J. Fluid Mech.* **283** 141-173
[9] Cossali G E, Coghe A and Marengo M 1997 *Exp. Fluids* **22** 463-472
[10] Roisman I V, Araneo L., Marengo M. and Tropea C 1999 *ILASS Europe*
[11] Panão M R and Moreira A L N 2002 *18th A. Conf. Liquid Atom. Spray Systems* 151-156
[12] Panão M R and Moreira A L N 2002 *SAE Technical Paper* 2002-01-2664
[13] Yanta W J and Smith R A 1978 *AIAA paper 73-169*
[14] Tates R W 1982, *ICLASS-82,* Wisconsin, USA, 341 – 351.
[15] Zhao F-Q, Lai M-C, Amer A A and Dressler J L 1996 *Atom. and Sprays* **6** 461-483
[16] Preussner C, Döring C, Fehler S and Kampmann S 1998 *SAE Technical Paper* Nº980498
[17] Meingast U, Staudt M, Reichelt L and Renz U 2000 *SAE Technical Paper* 2000-01-0272
[18] Rusche H 1997 *PhD Thesis*
[19] Bai C X, Rusche H and Gosman A D 2002 *Atom. and Sprays* **12** 1-27